Complete analysis of Very Fast Transients in Layer-type Transformer Windings

M. Popov, L. van der Sluis, R.P.P. Smeets

***Abstract*— This paper deals with the measurement, modelling and simulation of very fast transient overvoltages in layer-type distribution transformer windings. Measurements were performed by applying a step impulse with 50 ns rise time on a single-phase test transformer equipped with measuring points along the winding. Voltages along the transformer windings were computed by applying multi-conductor transmission line theory for transformer layers. The secondary voltage of the transformer was simulated with another model implemented in ATP-EMTP which takes into account the surge capacitance between the primary and secondary transformer winding. It was found that, when an impulse with a short rise time is applied, internal resonance occurs, which results in a very high secondary voltage. The computations were verified by measurements.**

***Keywords:* Transformer, very fast transients, high-frequency model, ATP-EMTP.**

I. Introduction

THE short rise time of a surge prompted by a lightning or a switching impulse can cause deterioration in the insulation and ultimately lead to a dielectric breakdown. The severity of this process depends on several factors, such as the frequency at which the transformer is exposed to this type of surge, the system configuration, the specific application of the component etc. Distribution transformers and motors are exposed to fast surges if they are switched by circuit breakers. Multiple reignitions can occur during the switching of transformers and motors with vacuum circuit breakers (VCBs), because of the ability of VCBs to interrupt high-frequency currents. The development process of multiple reignitions has been traced in detail [1,2]. It has been shown that the problem is not caused by the VCB or the transformer, but by an interaction of both [3]. It is therefore imperative to ascertain the speed at which transient oscillations propagate inside the windings and the coils, and to identify the possible reason for the transformer failure.

In order to study the propagation of transients a model is needed which is able to simulate the voltage distribution along the transformer winding. In [4-7], techniques of lumped parameter models are presented. Recent publications have revealed that the type of transformer winding is important for the choice of transformer model. In [8], it was demonstrated that a hybrid model based on multi-conductor transmission line theory could be successfully applied to describe the wave propagation in large shell-type transformers. In [9,10], two types of models were presented for transformers with interleaved windings; one was based on multi-conductor transmission line theory, while another was based on the modal approach as described in [11]. The advantage of the latter model is that it lends itself to the use of existing simulation software such as EMTP. Models based on multi-conductor transmission line theory can be applied if a frequency analysis is used. This model is purely numerical and the losses and proximity effects, normally represented in a wide frequency range can be easily taken into account.

The paper presents an analysis of the calculated and measured voltages along the high-voltage winding. For this purpose, multi-conductor transmission line theory is applied. A surge-transferred voltage to the secondary side is analyzed by making use of an EMTP model. The computations are verified by laboratory measurements.

II. Test Transformer

A. Transformer description

To calculate the voltage transients in transformer windings, it is important to determine the transformer parameters with a higher accuracy. These parameters are the inductances, the capacitances and the frequency-dependent losses. The modelling approach depends heavily on the transformer construction and the type of the windings. The test transformer in this case is a single-phase layer-type oil transformer. Fig. 1 shows the transformer during production in the factory.

The primary transformer winding consists of layers with a certain number of turns; the secondary winding is made of foil-type layers. Both windings are set on one leg of the core. The transformer is equipped with special measuring points in the middle and at the end of the first layer of the transformer high-voltage side, and also at the end of the second layer.

This work was supported by the Dutch Scientific Foundation NWO-STW under Grant VENI, DET.6526.

M. Popov and L. van der Sluis are with Power Systems Laboratory, Delft University of Technology, Mekelweg 4,2628CD Delft, The Netherlands (e-mail: M.Popov@tudelft.nl, L.vanderSluis@tudelft.nl).

R. P. P. Smeets is with KEMA T&D Testing, Utrechtseweg 310, 6812 AR Arnhem and with the Department of Electrical Engineering, Eindhoven University of Technology, Eindhoven, The Netherlands (e-mail: Rene.Smeets@kema.com).

Presented at the International Conference on Power Systems Transients (IPST'07) in Lyon, France on June 4-7, 2007

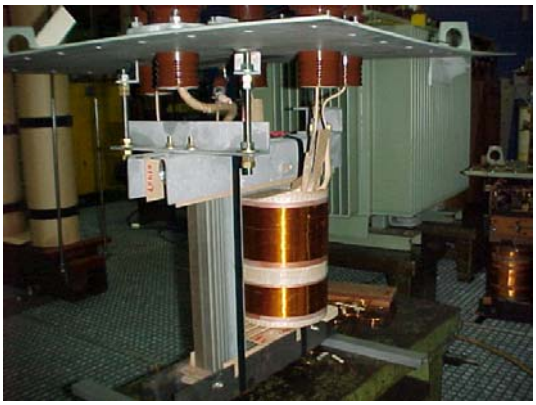

Fig. 1. Test transformer during production in the factory.

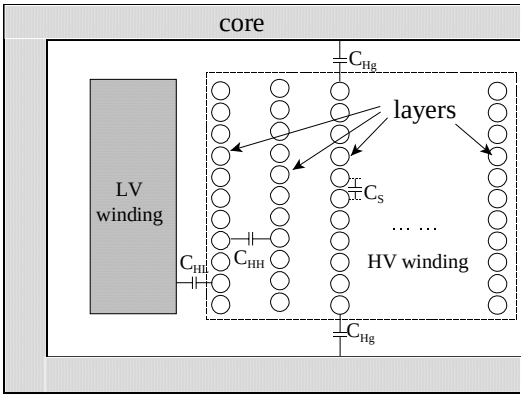

Fig. 2. Description of the capacitances inside a transformer.

TABLE I
TRANSFORMER DATA

Transformer Power	15 kVA
Transformer ratio	6600 V / 69 V
Short circuit voltage	310.3 V
Short circuit losses	332.5 W
No-load losses	57.2 W
No-load current	37.3 mA
Number of layers (HV side)	15
Number of turns in a layer	~ 200
Inner radius of HV winding	73.3 mm
External radius of HV winding	97.4 mm
Inner radius of the LV winding	51 mm
External radius of LV winding	67.8 mm
Wire diameter	1.16 mm
Double wire insulation	0.09 mm
Distance between layers	0.182 mm
Coil's height	250mm
Top / bottom distance from the core	10 mm
Dielectric Permittivity of oil	2.3
Dielectric Permittivity of wire insulation	4

All measuring points can be reached from the outside of the transformer and measurements can be performed directly at the layers. Table I shows the transformer data.

B. Determination of the transformer parameters

1) Capacitance

Fig. 2 shows the capacitances that are necessary for the computation of the fast transients inside the windings. These were calculated by using the basic formulas for plate and cylindrical capacitors. This is allowed because the layers and turns are so close to each other that the influence of the edges is negligible.

The capacitances C_S between the turns are important for the computation of transients in the turns. However, since the very large dimensions of the matrix prevent the voltages in each turn from being solved at one and the same time, a matrix reduction can be applied [12] so that the order of matrices corresponds not to a single turn but to a group of turns. In this way, the voltages at the end of the observed group of turns remain unchanged.

Capacitances C_{HH} between layers and capacitance C_{HL} between the primary and the secondary winding were calculated straightforward by treating the layers as a cylindrical capacitor.

The capacitances C_{Hg} to the ground are small in this case and estimated less than 1 pF. These are the capacitances from the layers to the core. We can see in Fig. 1 that only a part of the surface of the layers is at a short distance from the core and that it is mostly the geometry of the surface that influences the value of C_{Hg}. Another method is based on the extension of the width of the layer halfway into the barrier on the either side of the layer [7]. The capacitances to ground are the capacitances that govern the static voltage distribution.

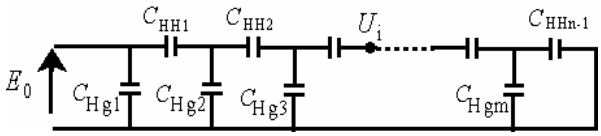

Fig. 3. A network for layer-to-layer static voltage distribution.

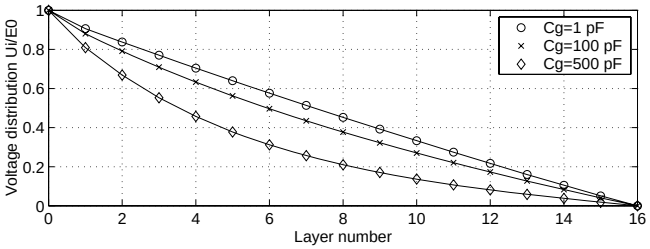

Fig. 4. Computed static voltage distribution for different grounding capacitances.

Fig. 4 shows the calculated static voltage distribution of each layer for a unit input voltage. When the ground capacitance in Fig. 3 is between 1 pF and 100 pF, the voltage distribution is more or less linear. The capacitances matrix **C** was formed as follows:

$C_{i,i}$ – is the capacitance of layer *i* to ground and the sum of all the other capacitances connected to layer *i*,

$C_{i,j}$ – is the capacitance between layers *i* and *j* taken with the negative sign ($i \neq j$).

The capacitance matrix has the diagonal, upper diagonal and lower diagonal elements non-zero values and all other elements are zeros.

2) Inductances

Inductances can be calculated by using the basic formulas for self- and mutual inductances of the turns, the so called Maxwell formulas.

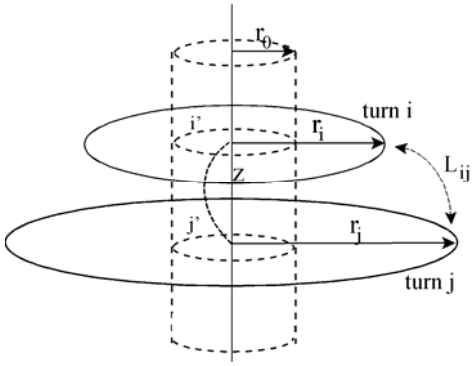

Fig. 5. Representation of circular turns for calculating inductances.

For turns as represented in Fig. 5, the self-inductance can be calculated as [13]:

$$L_{ii} = \mu_0 r_i \left(\ln \frac{16 r_i}{d} - 1.75 \right) \tag{1}$$

where r_i and d are the radius and the diameter of the turn. Radius r_i is calculated as a geometrical mean distance of the turn. The mutual inductances between turns *i* and *j* in Fig. 5 are obtained considering the two conductors as two ring wires:

$$L_{ij} = \mu_0 \sqrt{r_i r_j} \left(\left(\frac{2}{k} - k \right) K(k) - \frac{2}{k} E(k) \right) \tag{2}$$

where $k^2 = 4 r_i r_j / \left\{ (r_i + r_j)^2 + z^2 \right\}$; r_i, r_j and z are positions shown in Fig. 5; and $K(k)$ and $E(k)$ are complete elliptic integrals of the first and the second kind.

In this case, it is assume that the flux does not penetrate inside the core and a zero flux region exists. Therefore, the obtained self- and mutual inductances are compensated:

$$L_{ii} - L_{ii'} \text{ and } L_{ij} - 0.5(L_{ij'} + L_{i'j}). \tag{3}$$

The *i'* and *j'* are fictitious ring currents at zero flux region with radius r_0 with directions opposite to those of turns i and j. The method applied here holds for inductances on a turn-to-turn basis. The large matrix can be reduced applying a matrix reduction method based on the preservation of the same flux in the group of turns [12].

3) Copper and dielectric losses

Losses play an essential role in an accurate computation of the distributed voltages. The losses were calculated from the inductance matrix $\mathbf{L}$ and the capacitance matrix $\mathbf{C}$ [10]. The impedance and admittance matrices $\underline{Z}$ and $\underline{Y}$ are then:

$$\begin{aligned} \underline{Z} &= \left(j\omega + \sqrt{\frac{2\omega}{\sigma \mu_0 d^2}} \right) \mathbf{L} \\ \underline{Y} &= \left(j\omega + \omega \tan\delta \right) \mathbf{C} \end{aligned} \tag{4}$$

In (4), the second term in first equation corresponds to the Joule losses taking into account the skin effect in the copper conductor and the proximity effect. The second term in the second equation represents the dielectric losses. In (4),

d - is the distance between layers,

σ - is the conductor conductivity,

$\tan\delta$ - is the loss tangent of the insulation.

III. Modelling Approach

The transformer high-voltage winding is modelled by applying the Multi-conductor Transmission Line Modelling (MTLM). When a network of N coupled lines exists, then:

$$\begin{aligned} \frac{d^2 \underline{V}}{dx^2} &= -\underline{Z}\underline{Y}\underline{V} \\ \frac{d^2 \underline{I}}{dx^2} &= -\underline{Y}\underline{Z}\underline{I} \end{aligned} \tag{5}$$

where $\underline{Z}$ and $\underline{Y}$ are calculated according to (4). System equations (5) can be solved by making use of the modal analysis. This method is fully described in [14]. The time domain solutions are calculated by applying the continuous inverse Fourier Transform.

IV. Measurements and Simulations

Measurement equipment is shown in Fig. 6. The measuring terminals are on the top of the transformer lid. We can see in Fig. 2 that the transformer windings are actually connected to the transformer terminals by conductors with different parameters from those used for the transformer windings. These conductors are brought to the top of the transformer through conductive insulators, and as it can be seen from Fig. 2 they are passing close to the transformer core. The source voltage is not equal to the voltage at the first turn and the voltages measured at selected points have wave shapes that differ from the shape of the source voltage.

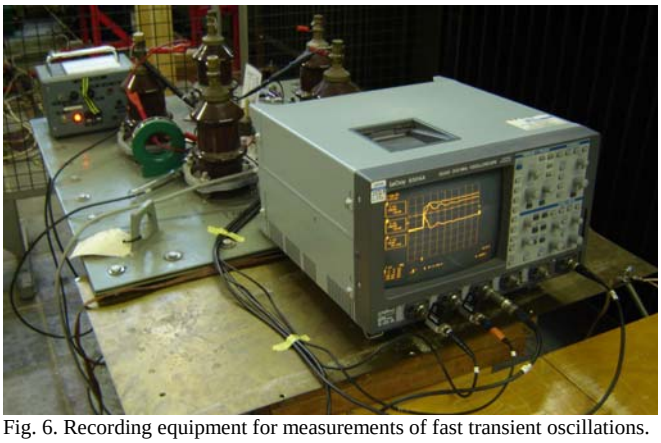

Fig. 6. Recording equipment for measurements of fast transient oscillations.

The applied model is valid only for the high-voltage transformer winding and not for the other connections that connect the transformer winding with the measuring points. So, the voltage at the first turn can therefore be estimated from Fig. 4, because the static voltage distribution is almost linear. Fig. 7 shows a comparison between the measured voltages and

the calculated voltages at the end of the first and second layer that correspond to the 200th and 400th turn respectively. Fig. 8 depicts computed voltages at the line-end coils of specific layers.

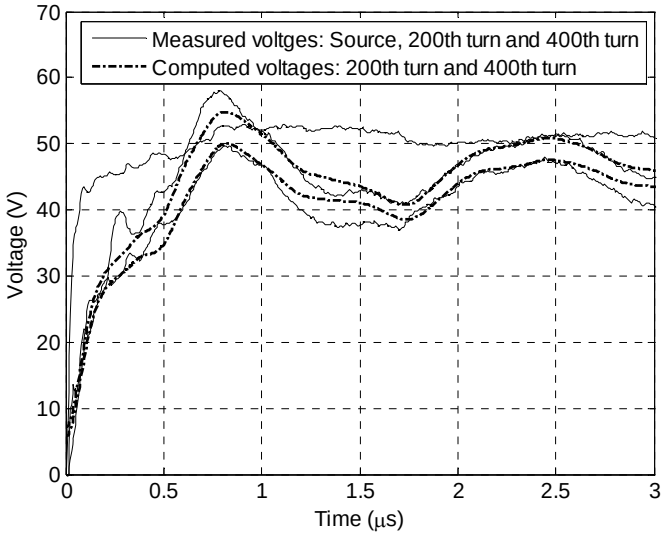

Fig. 7. Comparison between measured and computed voltage transients.

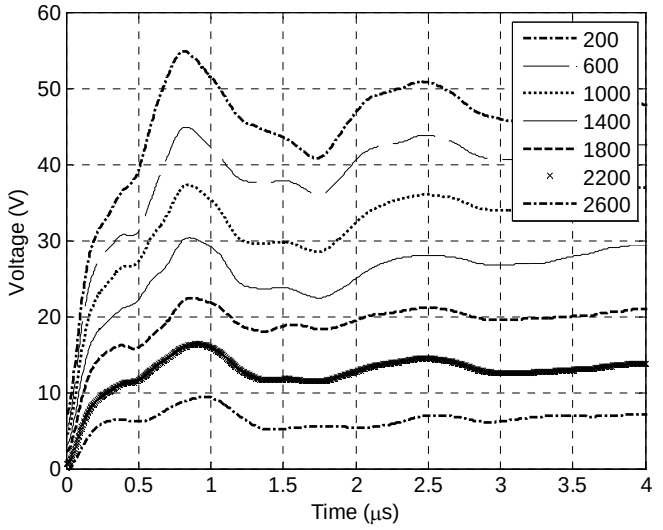

Fig. 8. Comparison between the calculated voltages at the 200th, 600th, 1000th, 1400th, 1800th, 2200th and 2600th turn.

V. Surge-Transferred Voltage Analysis

During fast voltage transients at the transformer primary terminals, high and steep voltages can be transferred to the transformer secondary side. These voltage values are much higher than voltages that occur under the normal operating conditions of the transformer. This is because the transformer secondary side voltage results from the inductive and the capacitive coupling between the primary and the secondary winding. At higher frequencies, the capacitive coupling has a dominant influence on the voltage amplitude and must not be neglected [15,16,17]. Terminal impedance characteristics on the primary and the secondary side were measured. Fig. 9 shows the amplitude and the phase terminal impedance characteristics for a no-loaded transformer and for a short-circuited transformer. This characteristic shows a resonant frequency below 1kHz (during no load). This frequency is outside the scope of this paper. It can be seen that, in the case of a short-circuited transformer, the resonant frequency moves to the right and downwards. This shows that the core has a significant influence for frequencies below 20 kHz. Above 20 kHz the two characteristics overlap.

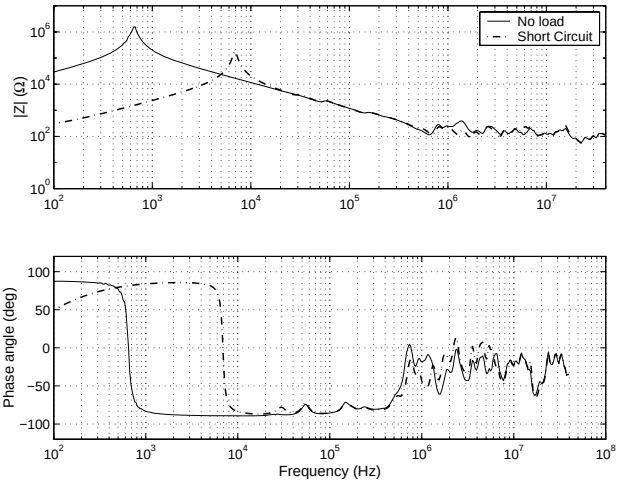

Fig. 9. Measured primary terminal impedance amplitude- and phase transformer characteristic for a transformer under no-load and for a short-circuited transformer.

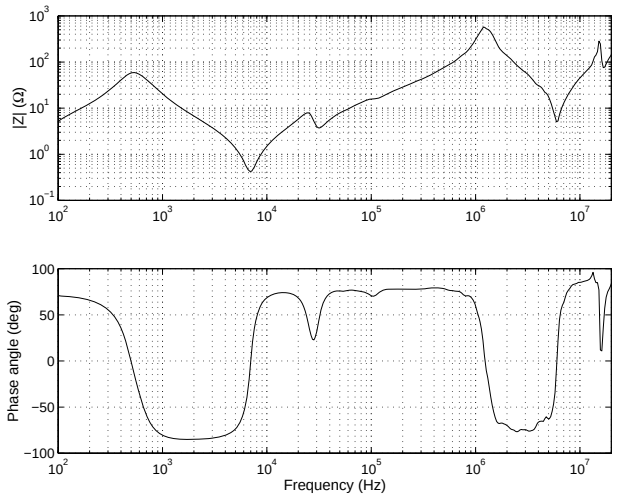

Fig. 10. Measured secondary terminal impedance amplitude- and phase transformer characteristic.

Terminal impedance characteristic for the low-voltage side when the high-voltage side is open is depicted in Fig. 10. For this transformer, the characteristic almost does not change when the high-voltage winding is closed. There are two resonant frequencies below 10 kHz and one resonant frequency around 1.3 MHz. The latter explains the occurrence of resonant overvoltages.

Fig. 11 shows a model of the transformer [15,16], which is applied for simulation of the surge transfer. This model is valid *only* for an analysis of the terminal voltages.

The parameters of the test transformer are listed in Table II. Since the transformer windings are built up in layers, the capacitances were calculated assuming the geometry of cylindrical capacitors. The crossover capacitance is the capacitance between the primary and the secondary winding. All other transformer data are provided by the manufacturer.

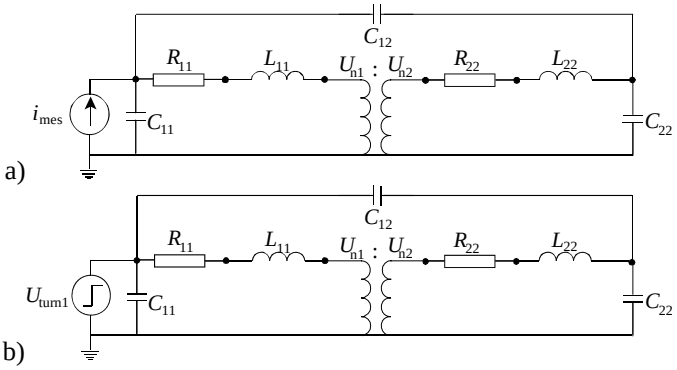

Fig. 11. Transformer model for analysing surge transfer based on: a) measured current; b) input first turn voltage.

TABLE II
PARAMETERS OF THE TRANSFORMER EQUIVALENT CIRCUIT

Leakage resistance R_{11}	128.8 Ω
Leakage inductance L_{11}	145.1 mH
Bushing capacitance C_{11}	1 nF
Leakage resistance R_{22}	0.003 Ω
Leakage inductance L_{22}	0.023 mH
Bushing capacitance C_{22}	0.22 nF
Iron-core losses R_m	750 kΩ
Cross-over capacitance C_{12}	0.41 nF

The transformer model is implemented in ATP-EMTP. Fig. 11a uses the measured source current while Fig. 11b uses the first-turn voltage. The sources are included in the ATP-EMTP by a point-list data file and a type-1 card. The point-list data file contains the measured points of the voltages and currents.

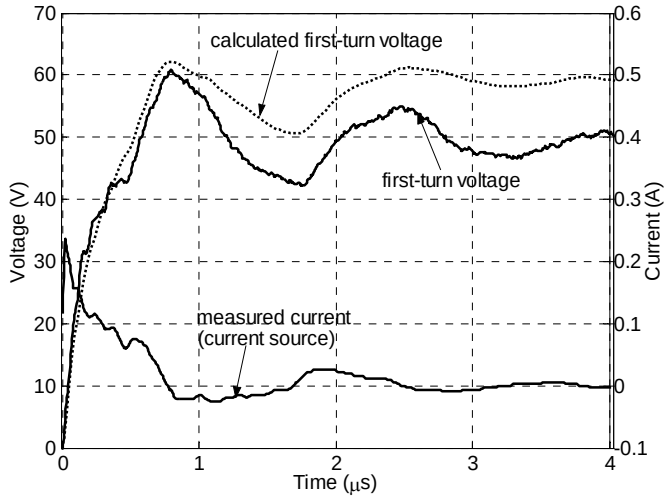

Fig. 12. Comparison of the actual and computed first-turn voltage when the measured current is taken as a current source.

Measured and computed results for both cases are depicted in Fig. 12 and Fig. 13. Fig. 12 shows the comparison between the actual and computed first-turn voltage at the high-voltage side when the measured current is used as excitation. The steepness of the calculated voltage more or less corresponds to that of the actual first-turn voltage. Fig. 13 shows the measured and calculated voltage at the secondary side. The values calculated with the model closely approximate the measured voltage.

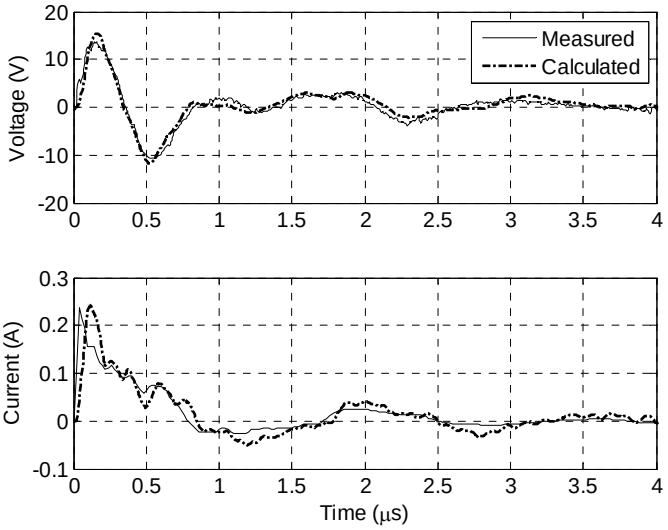

Fig. 13. Transformer model excited by the actual first-turn voltage;
1. Upper traces: measured and calculated voltage at the secondary terminal.
2. Lower traces: measured and calculated source current.

In Fig. 13, the source current is also calculated and compared with the originally measured current. Better results can be achieved by the model when a voltage source is used rather than a current source. The advantage of a current source is that it shows that the actual voltage at the first turn must not be similar to the voltage from the pulse generator.

VI. DISCUSSION

The study presented is an analysis of the voltage distribution along the high-voltage winding and an analysis of the surge-transferred voltage to the low-voltage winding. The voltages at the end of the first and the second layer were measured in a laboratory and simulated by applying the MTLM. From the measurements of the terminal impedance characteristic follows that no resonance frequencies in the high-frequency region for this particular transformer exist. Although no internal resonance was found on the high-voltage winding, for other transformers it might occur.

This study presents the worst-case scenario, when a steep surge is applied directly to the transformer terminal. This scenario could conceivably occur in, for instance, arc furnace systems, where the transformer is positioned close to the switchgear. When a cable is connected to the primary transformer side, the voltages will probably be less steep than in the case presented here.

VII. CONCLUSION

Modelling of layer-type distribution transformers by representing the turns and layers by transmission lines has been performed. The applied method is sufficient for computation of the voltages along the turns and layers when the inductance matrix $\mathbf{L}$ and capacitance matrix $\mathbf{C}$ are accurately determined. Inductance matrix is computed on a turn-to-turn basis with the traditionally known Maxwell formulas.

In the analysis, the proximity losses are taken into account so that the **R** matrix is not diagonal. This way of representing the inductances and losses is sufficient for very fast transients up to a few microseconds. To observe transients with longer period of time, which have oscillations with different frequencies like restrikes in the circuit breakers during switching transformers, the influence of the frequency-dependent core losses must be taken into account. The surge-transferred voltage has been measured and calculated by applying a simplified model that can be easily made in ATP-EMTP. Additional work should be done to investigate the voltage distribution in the low-voltage winding.

VIII. Acknowledgements

We wish to thank Dr. Jan Declercq and Ir. Hans de Herdt from Pauwels Transformers. We are also indebted to Kema High Voltage Laboratories and the High Current Laboratory at Eindhoven University of Technology for supplying the necessary equipment and for the use of their facilities, to Ir. R. Kerkenaar and Dr. A.P.J. van Deursen for their assistance in performing measurements of fast transients, and to Dr. J.L. Guardado from ITM, Morelia, Mexico, for acting as a discussion partner.

IX. References

[1] M. Popov, L. van der Sluis, G.C. Paap: "Investigation of the Circuit Breaker Reignition Overvoltages Caused by No-load Transformer Switching Surges", *European Trans.on Electric Power* (*ETEP*), Vol. 11, No. 6, November/December 2001, pp. 413-422.

[2] M. Popov, L. van der Sluis: "Improved Calculations for No-load Transformer Switching Surges, *IEEE Trans. on Power Delivery*, Vol.16, No.3, July 2001, pp. 401-408.

[3] J. Lopez-Roldan, H. de Herdt, T. Sels, D. van Dommelen, M. Popov, L. van der Sluis, J. Declercq: "Analysis, Simulation and Testing of Transformer Insulation Failures Related to Switching Transients Overvoltages", presented at CIGRE, paper 12-116, Paris, 2002.

[4] R.C. Degeneff, W.J. McNutt, W. Neugebauer, J. Panek, M.E. McCallum, C.C. Honey: "Transformer Response to System Switching Voltage", *IEEE Trans. on Power Apparatus and Systems*, Volume PAS-101, No.6, June 1982, pp. 1457-1470.

[5] M. Gutierrez, R.C. Degeneff, P.J. McKenny, J.M. Schneider: "Linear Lumped Parameter Transformer Model Reduction Technique", *IEEE Trans. on Power Delivery*, Vol.10, No.2, April 1995, pp. 853-861.

[6] M. Gutierrez, R.C. Degeneff, P.J. McKenny: "A Method for Constructing Reduced Order Models for System Studies from Detailed Lumped Parameter Models", *IEEE Trans. on Power Delivery*, Vol.7, No.2, April 1992, pp. 649-655.

[7] R.C. Dugan, R. Gabrick, J.C. Wright, K.V. Pattern: "Validated Techniques for Modeling Shell-form EHV Transformers", *IEEE Trans. on Power Delivery*, Vol.4, No.2, April 1989, pp. 1070-1078.

[8] M. Popov, L. van der Sluis, G.C. Paap, H. de Herdt: "Computation of Very Fast Transient Overvoltages in Transformer Windings", *IEEE Trans. on Power Delivery*, Vol. 18, no. 4, October 2003, pp. 1268-1274.

[9] K.J. Cornick, B. Fillat, C. Kieny, W. Müller: "Distribution of Very Fast Transient Overvoltages in Transformer Windings", presented at CIGRE, paper 12-204, Paris, 1992.

[10] Y. Shibuja, S. Fujita: "High Frequency Model of Transformer Winding", *Electrical Engineering in Japan*, Vol. 146, no.3, 2004, pp. 8-15.

[11] D.J. Wilcox, W.G. Hurleay, T.P. McHale, M. Conion: "Application of Modified Modal Theory in the Modeling of Practical Transformers", *Proceedings of IEE*, vol.139 Pt. C (6), pp. 513-520, 1992.

[12] F. de Leon, A. Semlyen: "Reduced Order Model for Transformer Transients", *IEEE Trans. on Power Delivery*, Vol. 7, no. 1, January 1992, pp. 361-369.

[13] F. Grover: "*Inductance Calculation: Working Formulas and Tables*", Dover Publication, New York, 1946, ISBN 0-87664-557-0.

[14] M. Popov, L. van der Sluis, R.P.P. Smeets, J. Lopez-Roldan: "Analysis of Very Fast Transients in Layer-type Transformer Windings", *IEEE Trans. on Power Delivery*, Vol.22, No.1, January 2007, pp. 238-247.

[15] A. Ametani, N. Kuroda, T. Tanimizu , H. Hasegawa, H. Inaba: "Field test and EMTP simulation of transient voltage when clearing a transformer secondary fault", *IEEJ Trans.*, Vol. B-118 (4), pp. 381-388, April 1998.

[16] A. Ametani, N. Kuroda, T. Tanimizu, H. Hasegawa, H. Inaba: "Theoretical analysis of transient recovery voltage when clearing a transformer secondary fault", *Electrical Engineering of Japan*, Vol. 134(3), pp. 44-52, 2001.

[17] IEC60076-3: "Power Transformers: Part 3 - Insulation Levels, Dielectric Tests and External Clearances in Air", http://www.iec.ch, IEC 2000.

X. Biographies

Marjan Popov (Member 1995; Senior Member 2003) graduated with a Dipl.-Ing. and M.S. in Electrical Engineering from the Sts. Cyril and Methodius University in 1993 and 1998 respectively and gained a PhD at Delft University of Technology in 2002. From 1993 until 1998 he was a teaching and research assistant at the Faculty of Electrical Engineering at the University of Skopje, spending 1997 as a visiting researcher at the University of Liverpool. He is currently assistant professor in the Electrical Power Systems Group at the Power Systems Laboratory at Delft University of Technology. His research interests are in arc modelling, transients in power systems, parameter estimation and relay protection. Dr. Popov is a senior member of IEEE.

Lou van der Sluis (Member 1981; Senior Member 1986) was born in Geervliet (Netherlands) on July 10, 1950. He obtained his MSc in Electrical Engineering from Delft University of Technology in 1974. He joined the KEMA High Power Laboratory in 1977 as a test engineer and was involved in the development of a data acquisition system for the High Power Laboratory, computer calculations of test circuits and the analysis of test data by digital computer. He became a part-time professor in 1990 and, two years later, was appointed full-time professor in the Power Systems Department at Delft University of Technology. Prof. van der Sluis is a senior member of IEEE and former chairman of CC-03 of Cigre and Cired to study the transient recovery voltages in medium and high voltage networks. He is currently a member of Cigre WG A3-20 for modeling power systems components.

René Peter Paul Smeets (Member 1995, Senior Member 2002) graduated with an MSc in Physics from Eindhoven University of Technology (Netherlands) in 1981. He obtained a PhD at the same institution in 1987 for research on vacuum arcs. He remained at Eindhoven as an assistant professor until 1995. During 1991, he was with the Toshiba Corporation's Heavy Apparatus Engineering Laboratory in Kawasaki (Japan), and, in 1995, joined KEMA in Arnhem (Netherlands). At present, he manages the R&D activities of KEMA's High Power Laboratory. In 2001, he was appointed part-time professor at Eindhoven University of Technology. Prof. Smeets is a senior member of IEEE.